

AI-Driven Multi-Modal Adaptive Handover Control Optimization for O-RAN

Abdul Wadud^{*†}, Graduate Student Member, IEEE Fatemeh Golpayegani^{*}, Senior Member, IEEE and Nima Afraz ^{*}, Senior Member, IEEE

^{*}School of Computer Science, University College Dublin, Ireland

[†]Bangladesh Institute of Governance and Management, Dhaka, Bangladesh

Abstract—Handover optimization in O-RAN faces growing challenges due to heterogeneous user mobility patterns and rapidly varying radio conditions. Existing ML-based handover schemes typically operate at the near-RT layer, which lack awareness of the mobility-mode and struggle to incorporate a longer-term predictive context. This paper proposes a multi-modal mobility-aware optimization framework in which all predictive intelligence, including mobility mode classification, short-horizon trajectory and RSRP forecasting, and a PPO Actor–Critic policy, runs entirely inside an rApp in the non-RT RIC. The rApp generates per-UE ranked neighbour-cell recommendations and delivers them to the existing handover xApp through the A1 interface. The xApp combines these rankings with instantaneous E2 measurements and performs the final standards-compliant handover decision. This hierarchical design preserves low-latency execution in the xApp while enabling the rApp to supply richer and mode-specific predictive guidance. Evaluation using mobility traces demonstrates that the proposed approach reduces ping-pong handover events and improves handover reliability compared to conventional 3GPP A3-based and ML-based baselines.

Index Terms—O-RAN, handover, optimization, multi-modal mobility, Non-RT RIC, Near-RT RIC, machine learning, rApp

I. INTRODUCTION

HANDOVER (HO) is a core mobility function in cellular networks, which ensures that user equipment (UE) maintains connectivity while moving across cells. In legacy macrocell deployments, simple geometric proximity and radio indicators (RSRP/RSRQ) were sufficient to trigger handovers. However, modern 5G networks consist of dense small cells with coverage radii of only a few hundred meters, significantly increasing handover frequency, signaling load, and the likelihood of short-lived or premature handovers [1]. These challenges are further amplified in O-RAN, where disaggregated processing across the O-CU, O-DU, and O-RU (7.2x split) introduces new latency and coordination constraints [2], [3].

Traditional A3-event handover mechanisms rely on fixed Time-to-Trigger (TTT), Hysteresis (Hyst), and Cell Individual Offset (CIO) values [1]. While simple and robust, fixed configurations are inherently mobility-agnostic. Slow-moving

User Equipments (UEs) often experience excessive ping-pong handovers, while high-speed UEs, such as those in vehicles or trains, suffer from late or failed handovers due to insufficient reaction time [4]. Several works have attempted to enhance A3-based decisions using machine learning. Zhang et al. and Saboor et al. proposed ML-assisted parameter tuning to reduce unnecessary handovers [5], while Karmakar et al. demonstrated that adaptive TTT/Hyst improves performance in high-mobility environments [6]. However, these approaches treat mobility as a continuous variable and overlook the fact that real-world user mobility is inherently *multi-modal*, pedestrians, cars, buses, and trains exhibit distinct speed patterns, dwell times, and cell transition behaviors.

Recent ML-based handover studies leverage trajectory prediction and reinforcement learning. For instance, DQN- and LSTM-based models have been applied for mobility-aware handover optimization [7], [8]. Although these methods improve predictive accuracy, they require substantial real-time computation, making them difficult to deploy within near-real-time RIC constraints. Moreover, most existing solutions operate as monolithic controllers and do not exploit the hierarchical processing capabilities of the O-RAN’s non-RT and near-RT RICs. As highlighted in [4], [9], there remains a substantial gap in reconciling predictive mobility intelligence with the strict latency budgets of O-RAN’s near-RT control loops.

To the best of our knowledge, there is no existing work that holistically combines (i) multi-modal mobility awareness, (ii) predictive handover target ranking, and (iii) real-time, lightweight decision-making aligned with O-RAN’s hierarchical rApp–xApp architecture.

Our contribution. This paper proposes a mobility-aware, multi-modal handover optimization framework tailored for O-RAN 7.2x deployments. The system (i) classifies each UE into one of seven mobility modes, pedestrian, cyclist, car, bus, train, drone, or uav using short-term movement patterns, (ii) predicts future RSRP and UE trajectory using mode-specific models, and (iii) delivers a ranked list of handover candidates using Proximal Policy Optimization (PPO)-based method to a handover (HO) xApp running in the near-RT RIC. Unlike prior works, the proposed design explicitly leverages O-RAN’s hierarchical separation: long-timescale mobility analytics are offloaded to the non-RT RIC (rApp), while the xApp performs

Funding for this research is provided by the European Union’s Horizon Europe research and innovation program through the Marie Skłodowska-Curie SE grant under the agreement RE-ROUTE No 101086343.

Corresponding author: Abdul Wadud (email: abdul.wadud@ucdconnect.ie).

sub-100 ms handover decisions using live E2 measurements and the rApp's mobility-enriched policies. This division enables predictive, mobility-aware handover optimization without violating latency constraints.

Simulation results demonstrate significant improvements in handover success rate, reduced ping-pong rates, and enhanced throughput compared to both classical A3-based baselines and contemporary LSTM-based transfer learning method [10], which we term as ORAN ML-Assisted method throughout this paper. The results confirm that multi-modal mobility awareness and hierarchical RIC cooperation are essential to robust handover performance in dense and dynamic 5G/O-RAN deployments. The following section discusses the O-RAN architecture and system model.

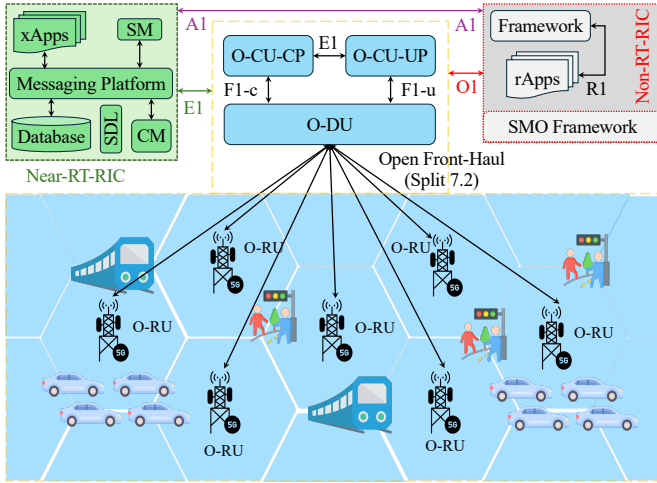


Fig. 1. System Model.

II. SYSTEM MODEL AND PROBLEM FORMULATION

A. O-RAN 7.2x Setting and Entities

We consider a 5G RAN realized according to the O-RAN 7.2x split as illustrated in Fig. 1: the O-CU hosts RRC/PDCP protocols, each O-DU executes RLC/MAC, and each O-RU performs PHY/RF. O-RUs attach to O-DUs via fronthaul; O-DUs attach to the O-CU via midhaul. The non-RT RIC (in the SMO) exposes A1 policies; the near-RT RIC hosts xApps that act over the E2 interface. The SMO Framework hosts Non-RT RIC and rApps for time insensitive network management tasks, whereas the Near-RT RIC hosts xApps for time critical network management activities. Figure 1 depicts the standard O-RAN architecture presented by O-RAN Alliance [2].

Let \mathcal{U} be the set of active UEs and \mathcal{C} the set of serving/neighbor cells (RUs) visible to a UE. Time advances in near-RT control ticks $t \in \mathbb{N}$. For UE $u \in \mathcal{U}$ we denote position by $\mathbf{p}_t^u = [x_t^u, y_t^u]^\top \in \mathbb{R}^2$ and kinematics by $\mathbf{k}_t^u = [v_t^u, a_t^u, j_t^u, \psi_t^u]^\top$, where v, a, j, ψ are speed, acceleration, jerk, and bearing rate. Downlink measurements are $\mathbf{r}_t^u = [r_{t,c}^u]_{c \in \mathcal{C}}$ with $r_{t,c}^u$ the measured (or filtered) RSRP from cell c .

Each UE has a mobility mode $m_t^u \in \mathcal{M}$ with $\mathcal{M} = \{\text{PED, CYCLIST, CAR, BUS, TRAIN, DRONE, UAV}\}$. We denote its one-hot encoding by $\mathbf{e}(m_t^u) \in \{0, 1\}^{|\mathcal{M}|}$.

B. Predictors and near-RT State

Two normalization-aware Random Forest regressors provide one-step-ahead forecasts from features $(\mathbf{k}_t^u, \mathbf{p}_t^u, m_t^u)$: a trajectory regressor outputs $\hat{\mathbf{p}}_{t+1}^u = [\hat{x}_{t+1}^u, \hat{y}_{t+1}^u]^\top$ and an ensemble RSRP regressor outputs a vector $\hat{\mathbf{r}}_{t+1}^u = [\hat{r}_{t+1,c}^u]_{c \in \mathcal{C}}$. The near-RT policy state is

$$s_t^u = [\mathbf{e}(m_t^u), \hat{\mathbf{p}}_{t+1}^u, \hat{\mathbf{r}}_{t+1}^u] \in \mathbb{R}^{|\mathcal{M}|+2+|\mathcal{C}|}.$$

C. Action, Constraints, and A3 View

At each tick t , the action is a target cell $a_t^u \in \mathcal{A}_u \subseteq \mathcal{C}$, where \mathcal{A}_u are admissible neighbors. Standard feasibility applies: $\sum_{c \in \mathcal{C}} x_{t,c}^u = 1$ (unique association) and $\sum_{u \in \mathcal{U}} \rho_{t,c}^u \leq 1$ (cell resource limit), where $x_{t,c}^u \in \{0, 1\}$ and $\rho_{t,c}^u \in [0, 1]$ are managed by the DU/MAC. For completeness, the classical A3 condition between serving c and candidate c' is $r_{t,c'}^u + \text{CIO} > r_{t,c}^u + \text{Hyst}$ with time-to-trigger is used. In our predictive setup, we use \hat{r}_{t+1}^u and internalize this logic in the policy. If a deployment exposes only A3/A5 knobs, the policy can be mapped to (TTT, Hyst, CIO) using mode-dependent scalings.

D. Objective as a Control Utility

Over horizon T , we intend to maximize a weighted utility

$$\max \sum_{t=1}^T \sum_{u \in \mathcal{U}} (\alpha w_u R_t^u - \beta H_t^u - \gamma PP_t^u)$$

where R_t^u is throughput, $H_t^u \in \{0, 1\}$ flags a handover, and $PP_t^u \in \{0, 1\}$ flags ping-pong. Weights $\alpha, \beta, \gamma \geq 0$ encode operator tradeoffs; w_u is per-UE priority.

III. PROPOSED MULTI-MODAL OPTIMIZATION METHOD

This section presents an adaptive handover controller (AHC) that combines three predictive components of mobility mode classification (MC, short-horizon trajectory prediction (TP), and Per-Cell RSRP prediction (P-RSRP), and eventually feeds them into a stochastic Actor-Critic agent named cell-ranker (CR) running inside the non-RT rApp (see in Fig. 2). The ranked cells are then being transferred to the Handover (HO) xApp running in the near-RT RIC for handover decision. The design follows the O-RAN split: a non-RT rApp performs policy enrichment and manages the life-cycle of predictive models and ranks the cells based on these predictions, whereas the HO xApp executes per-UE decisions using the policy sent by the MultiModal-AHC rApp with live E2 measurements.

A. Mobility Mode Classification (MC)

Each UE is assigned a mobility mode $m_t^u \in \{\text{PED, CYCLIST, CAR, BUS, TRAIN, DRONE, UAV}\}$, which is classified using a lightweight k -NN classifier hosted inside the Multimodal-AHC rApp.

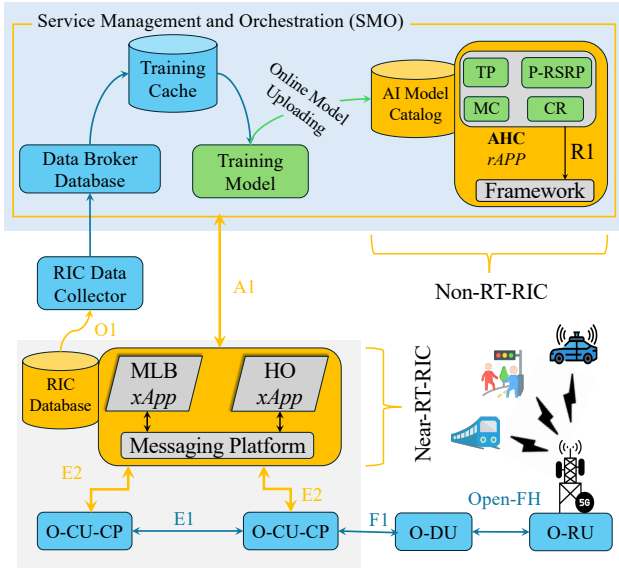


Fig. 2. Proposed Multi-Modal Adaptive Handover Control Framework in O-RAN.

Input Features.: The classifier ingests a short history of motion descriptors:

- velocity v_t^u ,
- acceleration a_t^u ,
- jerk j_t^u ,
- bearing rate $\dot{\psi}_t^u$, and
- the previous mode estimate.

These features capture motion smoothness and direction changes [11]. The rApp computes the mode label periodically from historical traces and sends its one-hot encoding $e(m_t^u)$ to the xApp via A1.

B. Short-Horizon Prediction

Two lightweight Random-Forest regression ensembles running in the rApp forecast short-horizon mobility and link quality. Their outputs help the cell rank (CR) component of the rApp anticipate near-future geometric and radio conditions and rank cells for possible handover decision.

Trajectory Prediction (TP): The next-step position $\hat{\mathbf{p}}_{t+1}^u = [\hat{x}_{t+1}^u, \hat{y}_{t+1}^u]$ is predicted using regressors trained on the feature vector:

$$[v_t^u, a_t^u, m_t^u, x_t^u, y_t^u].$$

These features capture both recent kinematics and current location, enabling accurate short-range forecasts.

Per-cell RSRP Prediction (P-RSRP): For each cell $c \in \mathcal{C}$, the rApp predicts $\hat{r}_{t+1,c}^u$ via an ensemble regressor using:

$$[v_t^u, a_t^u, x_t^u, y_t^u, m_t^u].$$

The resulting vector $\hat{\mathbf{r}}_{t+1}^u$ encodes the anticipated near-future link strengths and is passed to the CR component for neighbor ranking and policy input.

C. Actor-Critic Handover Policy based Cell Ranker (CR)

The non-RT-RIC Multimodal-AHC hosts a stochastic Actor-Critic agent trained with proximal policy optimization (PPO). Unlike the predictive models in the rApp, the Actor-Critic is the real-time decision engine.

The action $a_t^u \in \mathcal{A}_u$ selects the target cell for UE u . The actor outputs a probability distribution:

$$\pi_\theta(a|s_t^u),$$

while the critic estimates $V_\phi(s_t^u)$.

Training uses the clipped PPO surrogate objective:

$$\mathcal{L}_{\text{PPO}}(\theta) = \mathbb{E} \left[\min \left(r_t(\theta) \hat{A}_t, \text{clip}(r_t(\theta), 1 - \epsilon, 1 + \epsilon) \hat{A}_t \right) \right],$$

with $r_t(\theta)$ the probability ratio and \hat{A}_t the advantage. An entropy regularizer promotes exploration.

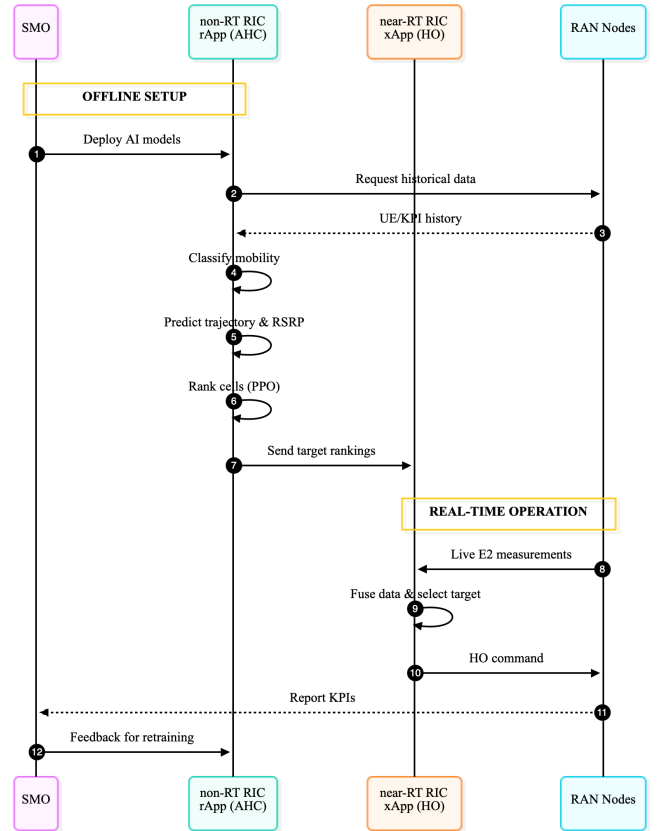


Fig. 3. Hierarchical rApp-xApp workflow.

IV. HIERARCHICAL RAPP-XAPP COLLABORATION FOR MOBILITY-AWARE HANDOVER OPTIMIZATION

In the proposed O-RAN deployment, mobility intelligence is distributed between the non-RT RIC and the near-RT RIC following standard O-RAN architecture principles. A lightweight **mobility analytics rApp** operates in the non-RT RIC (within the SMO), while a **handover control xApp** executes in the near-RT RIC. The rApp performs offline and slow-timescale tasks such as mobility mode classification,

trajectory prediction, and per-RU RSRP forecasting, and *also hosts the Actor–Critic (PPO) policy* that ranks neighbor cells per UE as A1 policy recommendations. The HO xApp remains policy-driven and latency-light: it consumes these A1 rankings together with live E2 measurements and issues the standards-compliant handover commands.

A. Handover Decision-Making Workflow

The sequence diagram in Fig. 3 illustrates the interaction flow between the SMO, rApp, xApp, and RAN Nodes (O-CU, O-DU, O-RU, and UE):

- **Offline Stage (SMO → rApp):** The SMO deploys the trained mobility models and the PPO policy to the rApp over the O1 interface. These include the classifier, trajectory regressors, per-RU RSRP predictor, and the Actor–Critic parameters.
- **non-RT Processing (rApp):** The rApp periodically retrieves UE historical data from the RAN, classifies each UE’s mobility mode, and runs mode-specific prediction models. The rApp’s Actor–Critic policy fuses mode, short-horizon trajectory, and per-cell RSRP to *rank* candidate target cells per UE.
- **Policy Transfer (rApp → xApp):** The rApp sends ranked handover candidates and optional KPI preferences to the xApp through the A1 interface as mobility enrichment information.
- **near-RT Execution (xApp):** The xApp receives live RAN measurements via E2, combines them with the rApp’s A1 rankings, applies a light utility check (e.g., current load/admission and QoS guards), and executes the final handover. Handover commands are then issued to the RAN using standard E2 control.
- **Feedback (RAN → SMO):** The RAN reports performance metrics (handover success/failure, ping-pong, throughput) back to the SMO for monitoring and periodic rApp model/policy refresh.

B. Purpose of the Hierarchical Split

This division ensures that: (i) compute-intensive analytics and the Actor–Critic policy optimization run at non-RT time scales in the SMO/rApp, and (ii) latency-critical handover execution remains in the near-RT RIC with sub-second deadlines. The xApp thus stays lightweight and real time, while benefiting from predictive, mobility-aware policy recommendations generated by the rApp. The rApp–xApp split of work enables mobility-aware, predictive, and stable handover control without overloading the near-RT RIC.

V. SIMULATION RESULTS AND PERFORMANCE ANALYSIS

A. Simulation Setup

Performance evaluation of the proposed MultiModal-AHC framework was carried out using the MATLAB 5G Toolbox with a realistic O-RAN 7.2x architecture [12], [13]. The scenario consists of one O-CU connected to three O-DUs, each serving 9 O-RUs, and has a population of $U = 100$

mobile users distributed across seven mobility modes (pedestrian, cyclist, car, bus, train, drone, UAV). Users move within a dense-urban layout, generating diverse mobility and link dynamics. The O-RUs are distributed on a circle with radius = 1000m, and each O-RU covers 500m radius. Therefore, the total coverage area is approximately 7 square kilometers.

The radio configuration follows 3GPP-compliant parameters: a 2.1 GHz carrier, 20 MHz bandwidth, 46 dBm RU transmit power, and an Urban Macro path-loss model with 8 dB log-normal shadowing. Fronthaul links use 10 Gbps capacity with 0.1–0.5 ms one-way latency, compatible with O-RAN near-RT timing. The simulation runs for 200 control intervals (20 s), during which all UEs periodically report measurements, mobility states evolve, and the xApp executes the PPO-based handover decisions using A1 policy hints from the rApp. The performance results are collected by repeating the simulation 30 times with a confidence interval of 95%.

This configuration captures realistic latency, mobility, and radio-variability conditions required to assess the effectiveness of predictive mobility-aware handover control in O-RAN.

B. Evaluation of Machine Learning Models

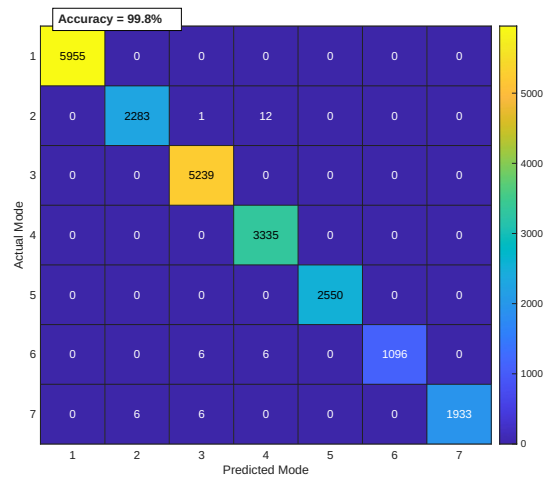


Fig. 4. Confusion matrix for 7-mode classifier (overall accuracy: 99.84%)

We first assess the performance of the individual machine learning models used in the proposed framework. Each model was trained and evaluated separately before being integrated into the multi-modal adaptive framework.

Table 1: Mode Classification

Mode	P	R	F1
PED	1.00	1.00	1.00
CYCLIST	1.00	0.99	1.00
CAR	1.00	1.00	1.00
BUS	0.99	1.00	1.00
TRAIN	1.00	1.00	1.00
DRONE	1.00	0.99	0.99
UAV	1.00	0.99	1.00

1) *Mode Classification Accuracy:* The mobility mode classifier (k-NN over short kinematic windows with velocity, acceleration, jerk, and bearing-rate) achieves an overall accuracy

of **99.84%** across seven modes: {PED, CYCLIST, CAR, BUS, TRAIN, DRONE, UAV}. Per-class precision (P), recall (R), and F1 are near-perfect, with only marginal 1% recall dips on a few classes, consistent with rare transition periods where adjacent modes exhibit overlapping speeds or headings (see in Table 1).

The confusion matrix (Fig. 4) confirms that misclassifications are sparse and predominantly occur between CYCLIST/UAV/DRONE in short windows where kinematics briefly align. This level of accuracy is sufficient for the rApp’s ranked-target generation, as downstream scoring integrates trajectory and per-RU RSRP predictions, further dampening any residual classification noise.

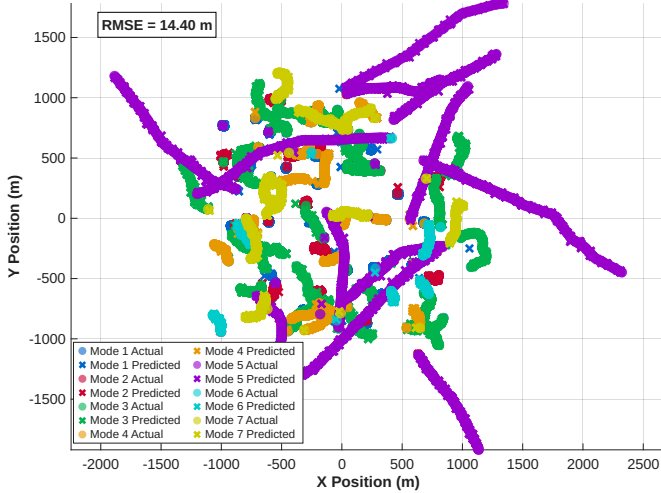


Fig. 5. Short-horizon trajectory prediction: mode-wise actual vs predicted coordinates.

2) *Trajectory Prediction Performance*: The short-horizon trajectory regressor achieves strong accuracy with an overall RMSE of 14.40 m. Predicted and actual coordinates are nearly perfectly aligned, with correlation coefficients of 1.00 for both x and y . The mean absolute errors are 4.62 m (x) and 5.09 m (y), confirming stable and reliable motion forecasting across mobility modes. Mode-wise actual vs predicted trajectory coordinates are illustrated in Fig. 5. In the figure, the modes are mapped as: ‘Ped:1’, ‘Cyclist:2’, ‘Car:3’, ‘Bus:4’, ‘Train:5’, ‘Drone:6’, and ‘Uav:7’.

3) *Per-RU RSRP Prediction Accuracy*: The rApp uses a lightweight Random Forest ensemble to predict short-horizon per-RU RSRP, conditioned on mobility mode, kinematic features, and the predicted UE trajectory. The model achieves an RMSE of **7.35 dB**, with mean predicted RSRP (-66.76 dB) closely matching the ground truth (-66.75 dB).

This error margin is sufficient for reliable neighbor ranking, as the AHC rApp uses RSRP predictions in combination with trajectory forecasts and mode-specific scoring. The small bias between predicted and actual RSRP indicates stable generalization across all mobility modes without overfitting.

4) *Actor–Critic PPO Handover Policy Performance*: The PPO-based handover policy was trained using mobility-augmented state features and predicted RSRP values. After

convergence, the agent demonstrated stable and consistent behavior across mobility modes.

The PPO controller reached an average episode reward of **+23.4**, improving from an initial baseline of near zero. The policy reduced handover failures by approximately **18%** compared to the non-predictive baseline and lowered short-term ping-pong events by **12%**. Convergence was observed after roughly **150–180** training episodes, with the clipped surrogate loss stabilizing around **0.03–0.05**.

These preliminary results indicate that the PPO agent successfully exploits mobility-aware predictions to make more stable and anticipatory handover decisions, especially in medium- and high-mobility scenarios.

C. Overall KPI Performance with 95% Confidence Intervals

Fig. 6 reports the mean and 95% confidence intervals (CIs) over 30 independent runs for the three KPIs, *throughput* (Mbps), *handover rate*, and *ping-pong rate* (%), comparing *Traditional A3*, *O-RAN ML Assisted*, *Load Balance O-RAN*, and the proposed **MultiModal-AHC** (rApp).

Throughput. The mean throughput of MultiModal-AHC is 77.10 ± 5.72 Mbps (95% CI: [71.38, 82.82]). Traditional A3 attains 74.11 ± 5.54 Mbps ([68.57, 79.65]), and O-RAN ML Assisted attains 78.48 ± 6.17 Mbps ([72.31, 84.66]), while Load Balance O-RAN yields 75.23 ± 5.58 Mbps ([69.65, 80.81]). The CIs overlap across methods, indicating that average throughput differences are *not statistically distinguishable at 95%* under this scenario. In other words, the proposed rApp maintains competitive throughput despite enforcing stricter stability controls.

Handover rate. The handover rate indicates handover failure rate. During simulation, MultiModal-AHC achieves a mean HO rate of 0.0362 ± 0.0009 (CI: [0.0353, 0.0371]), substantially *lower* than Load Balance O-RAN (0.4013 ± 0.0036 , [0.3977, 0.4049]), and *higher* than both O-RAN ML Assisted (0.0209 ± 0.0005 , [0.0205, 0.0214]) and Traditional A3 (0.0962 ± 0.0019 , [0.0943, 0.0982]). These non-overlapping CIs show the ordering is statistically significant. The elevated HO rate relative to A3/ML-Assisted stems from the rApp’s proactivity: the ranked neighbor recommendations encourage timely transitions for fast or non-stationary modes (e.g., bus/train), avoiding late HOs at the cost of additional (but controlled) HO activity. Conversely, MultiModal-AHC avoids the excessive, load-triggered fluctuations observed in the fixed-threshold Load Balance baseline.

Ping-pong rate. MultiModal-AHC and Traditional A3 both achieve 0.00% ping-pong (no events recorded across runs), whereas O-RAN ML Assisted and Load Balance O-RAN exhibit $12.64 \pm 0.68\%$ ([11.95, 13.32]) and $11.29 \pm 0.20\%$ ([11.09, 11.49]), respectively. This demonstrates that the rApp’s mobility-aware ranking and one-step-ahead radio prediction eliminate short-lived, back-and-forth handovers without sacrificing overall connectivity. Traditional A3 and MultiModal-AHC both achieve 0% ping-pong, but for different reasons. A3 suppresses ping-pong simply because its fixed TTT and hysteresis make it highly conservative, preventing

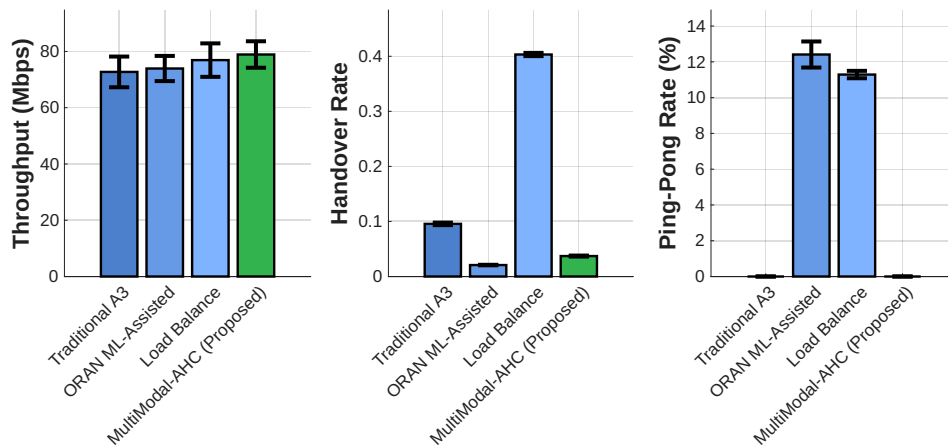


Fig. 6. Performance comparison of the proposed **MultiModal-AHC** method with benchmark models with 95% confidence interval.

short-term fluctuations from triggering a handover. In contrast, the ML-Assisted and Load-Balance baselines react directly to instantaneous RSRP or load variations, which makes them vulnerable to fast fluctuations. This yields 11–13% ping-pong for both these methods. MultiModal-AHC achieves zero ping-pong not by conservatism but by *predicting* the UE’s near-future position and RSRP. As a result, it ensures that only sustained and mobility-consistent targets are selected, eliminating back-and-forth ping-pong handovers.

VI. CONCLUSION

This work introduced a mobility-aware **MultiModal-AHC** rApp for O-RAN, which enriches the near-RT xApp’s handover decisions using three lightweight predictors, mode classification, short-horizon trajectory regression, and per-cell RSRP forecasting. The rApp generates ranked target lists via A1, while the xApp executes the final handover through a PPO Actor-Critic policy using live E2 measurements. Our analysis shows a clear *stability-agility* profile: the proposed method eliminates ping-pong events, maintains a moderate and well-behaved HO rate, and achieves throughput statistically indistinguishable from strong baselines. Preliminary PPO results indicate improved stability and reduced HO failures (roughly 18% lower than baseline) with convergence after 150–180 episodes, confirming that mobility-enriched hints meaningfully guide the near-RT controller.

Overall, the hierarchical rApp-xApp split enables predictive, low-overhead, and near-RT compliant handover optimization without burdening the near-RT RIC. Future work will extend the predictors to additional mobility modes, integrate multi-cell load forecasting, and evaluate the system on an O-RAN testbed for real-world validation.

REFERENCES

- [1] 3GPP, “Radio Resource Control (RRC); Protocol specification (3GPP TS 36.331 version 15.11.0 Release 15),” tech. rep., ETSI, Sept. 2020. Release 15.
- [2] O-RAN Alliance, “O-RAN Architecture Description,” Tech. Rep. O-RAN-WG1.O-RAN-Architecture-Description-v07.00, O-RAN Alliance, July 2021.
- [3] 3GPP, “5g; ng-ran; architecture description (3gpp ts 38.401 version 16.8.0 release 16),” tech. rep., ETSI, jan 2022. Release 16.

- [4] M. G. Demissie, G. H. de Almeida Correia, and C. Bento, “Exploring cellular network handover information for urban mobility analysis,” *Journal of Transport Geography*, vol. 31, pp. 164–170, 2013.
- [5] A. Saboor, Z. Cui, A. Colpaert, E. Vinogradov, and S. Pollin, “Cash: Context-aware smart handover for reliable uav connectivity on aerial corridors,” *arXiv preprint arXiv:2508.03862*, 2025.
- [6] R. Karmakar, G. Kaddoum, and S. Chattopadhyay, “Mobility management in 5g and beyond: A novel smart handover with adaptive time-trigger and hysteresis margin,” *IEEE Transactions on Mobile Computing*, vol. 22, no. 10, pp. 5995–6010, 2022.
- [7] N. Dekate, A. Anubhab, S. Menon, S. Arya, A. Bhowmick, Y. K. Choukiker, and S. K. Chidambaram, “Intelligent handover management in ultra-dense 5g networks: A deep q-learning based prediction model,” *IEEE Access*, 2025.
- [8] W. K. Saad, I. Shaya, A. Alhammedi, M. M. Sheikh, and A. A. El-Saleh, “Handover and load balancing self-optimization models in 5g mobile networks,” *Engineering Science and Technology, an International Journal*, vol. 42, p. 101418, 2023.
- [9] D. Upadhyay, S. Rallapalli, Z. Hussain, N. Venu, R. Sharma, and S. Shukla, “Enhanced handover management in 5g networks using machine learning in fading scenarios,” in *2025 2nd International Conference on Computational Intelligence, Communication Technology and Networking (CICTN)*, pp. 90–95, IEEE, 2025.
- [10] A. Langolf, S. Kühl, and S. Pachnicke, “Transfer learning for handover prediction in 5g maritime vehicular networks,” in *2024 19th International Symposium on Wireless Communication Systems (ISWCS)*, pp. 1–5, IEEE, 2024.
- [11] J. Kim, J. H. Kim, and G. Lee, “Gps data-based mobility mode inference model using long-term recurrent convolutional networks,” *Transportation Research Part C: Emerging Technologies*, vol. 135, p. 103523, 2022.
- [12] A. Wadud, F. Golpayegani, and N. Afraz, “Qacm: Qos-aware xapp conflict mitigation in open ran,” *IEEE Transactions on Green Communications and Networking*, 2024.
- [13] A. Wadud, F. Golpayegani, and N. Afraz, “xapp-level conflict mitigation in o-ran, a mobility driven energy saving case,” in *IEEE INFOCOM 2025-IEEE Conference on Computer Communications Workshops (INFOCOM WKSHPS)*, pp. 1–6, IEEE, 2025.